Macromolecules

ARTICLE

pubs.acs.org/Macromolecules

Segmental Dynamics and Ion Association in PEO-Based Single Ion Conductors

Kokonad Sinha and Janna K. Maranas*

Department of Chemical Engineering, The Pennsylvania State University, University Park, Pennsylvania 16802, United States

ABSTRACT: We use quasi-elastic neutron scattering (QENS) to characterize polymer dynamics in solid polymer electrolytes (SPEs) that function as single ion conductors. In this case, the SPE combines a PEO spacer with a comonomer that introduces an acid group that serves as the anion. In these single ion conductors (ionomers), only the cation is not covalently bonded to the polymer chain. We study polymer dynamics as a function of ion content, as controlled by varying the ratio of nonionized to ionized comonomers. Even in nonionic polymers (no acid groups), we observe two segmental processes, which we interpret as motion of PEO segments in the spacer midpoint and near the isophthalate groups. In ionized samples, cross-linking between ionic groups considerably slows the dynamics of PEO segments near the isophthalate group. We compare the results to the PEO/$LiClO_4$ system by comparing both polymer dynamics and conductivity as a function of ion content. The optimal ion content for ionomers is half that of the salt system, which we explain based on the differing behavior of polymer dynamics in the two systems.

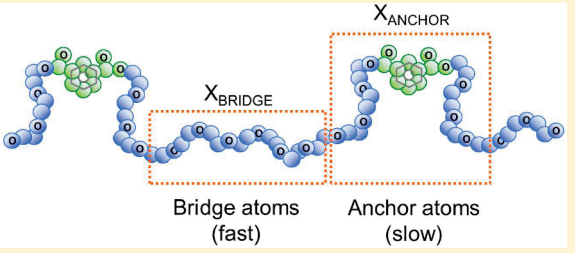

INTRODUCTION

Lithium ion batteries are extensively used in portable devices because they are rechargeable and have high energy density. Liquid electrolytes used in these batteries are toxic and require a hard casing that limits flexibility. Scientists are therefore turning to the use of nontoxic solid polymer electrolytes (SPEs), which alleviate these difficulties. SPEs require a polymer host and a cation source such as lithium salt. Poly(ethylene oxide) (PEO) is frequently chosen as the polymer host because it has the ability to solvate the cation with its ether oxygen atoms. The cation moves through the polymer by making and breaking bonds with the ether oxygen atoms.[1−4] However, the rate at which lithium ions move at room temperature is low, resulting in ionic conductivity that is insufficient for practical application. Because both anions and cations are mobile, accumulation of unwanted charge can occur at the electrodes. This degrades battery performance, and therefore, an electrolyte in which the cation is the only conducting element is desirable.[5,6]

One material in which the cation is the only conducting element is the "single ion conductor",[7−20] where the anion is covalently bonded to the polymer chain so that the transference number is unity. They belong to a class of systems called ionomers. The ion content in ionomers is related to the number of anion bearing comonomers relative to the rest of the chain and is often limited for synthetic reasons to low values. In contrast to most ionomers, the nonionic part of the chain in PEO-based SPE single ion conductors can partially solvate the cations, such that the X-ray scattering associated with ionic aggregation is less prominent.[21] Single ion conductors suffer from low conductivity and excessive ion pairing. Though the conductivity can be improved by reducing the molecular weight, it results in poor mechanical properties. Although reducing the conducting species to only the cation should improve extraction of mechanistic information on ion transport, less is known about these materials than Li salt/PEO systems. A complicating factor compared to Li salt/PEO systems is the possibility of nanoscale ionic aggregation, which would involve the polymer chain, thus impacting cation solvation and polymer dynamics, both of which influence conductivity. This paper investigates segmental mobility of the polymer in PEO-based single ion conductors, specifically the influence of introducing the anion-bearing comonomer and varying ion concentration.

The study is a part of a collaboration investigating ionic transport in PEO-based single ion conductors. By combining results obtained from quasi-elastic neutron scattering (QENS), dielectric relaxation spectroscopy (DRS),[22−24] NMR, FTIR,[25] X-ray scattering,[21] *ab initio* calculations,[21] and molecular dynamics simulations, we address cation−polymer interactions through the interplay of dynamics, morphology, and ionic conductivity. We study systems where sulfonate groups (anions) are covalently bonded to a PEO chain by means of isophthalate groups, as shown in Figure 1. These systems allow us to change three variables: (a) the ratio of isophthalate groups ionized with SO_3^- to the overall number of isophthalate groups, called the degree of sulfonation (Y%); (b) the length of the polymer chain or the spacer unit (N); and (c) the identity of the cation. The degree of sulfonation and length of the spacer unit control the ion content of the sample. Variation of ion identity allows us to explore the effect of ion association energies on the cation−polymer interaction strength.

In the results presented here, we use a sodium cation with $N = 13$ (which corresponds to spacer MW = 600 g/mol) and vary

Received: March 4, 2011
Revised: May 29, 2011
Published: June 15, 2011

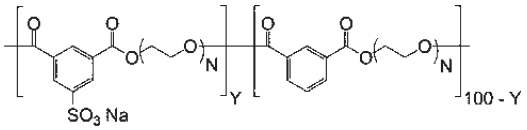

Figure 1. Chemical structure of PEO600-*Y*%Na.

Y from 0 to 100%. The corresponding nomenclature used is PEO600-*Y*%Na. We choose Na for this study because the Na ionomers do not microphase separate and are amorphous, single-phase materials in the temperature range of our study, whereas the Li ionomers show evidence of ion segregation at all temperatures.[21−24] Thus, the Na system is most similar to the Li/salt systems previously studied. We will consider the Li ionomers in a future publication. Small-angle X-ray scattering (SAXS) and DRS studies suggest that the ions in this system occupy a wide range of local environments, including small aggregates, ion pairs, and ions solvated by the PEO spacer. Ionic conductivity in amorphous solid polymer electrolytes (SPE) depends strongly on polymer mobility. For PEO/salt systems, lithium ions are solvated by the ether oxygen atoms on the PEO chains, which slows the segmental motion of the polymer.[1,2,26,27] A similar effect is expected for PEO-based single ion conductors, with some additional considerations. The presence of a comonomer every 13 PEO repeat units means that a significant fraction of the PEO spacer could be influenced by the comonomer, should its dynamics vary considerably from PEO. When ions are present, they may not solvate all parts of the PEO spacer equally (for example, they may prefer locations near the anions), leading to interesting changes in dynamics with ion content. Because polymer dynamics is tied to conductivity, it is important to understand these issues. QENS is an effective way to observe the dynamics of polymers and has previously been applied to pure PEO and PEO/Li−salt systems. The polymer mobility of SPEs above their melting temperature has been measured using QENS for PEO/LiI,[27] PEO/$LiClO_4$,[28,29] PEO/LiTFSI,[1] and PEO/$LiN(SO_2C_2F_5)_2$.[2,30] For all SPEs, the segmental mobility of PEO decreases with the addition of lithium salt because the lithium cations coordinate with multiple ether oxygen atoms. For those systems in which the most stable crystal phase is PEO_6 with six PEO ether oxygens for each Li ion [PEO/LiTFSI,[31] PEO/$LiClO_4$[32] and PEO/$LiN(SO_2C_2F_5)_2$[33]] a process additional to segmental relaxation was observed.[1,2,28,30,34,35] Some authors attribute this to the formation and breaking of "cross-links" between Li^+ and ether oxygen atoms.[2,35] Our study of the PEO/$LiClO_4$ system shows that the slower process is rotational in nature and related to remnants of the PEO_6 crystalline phase, which have been observed above T_m for PEO/$LiClO_4$[29] and other systems.[31,36]

Dielectric spectroscopy on the ionomers in this study[23,37] and poly(ethylene oxide)-based polyurethane ionomers[24] shows a slowing down of segmental dynamics with increasing ion content, reflected by the increase of the glass transition temperature. A relaxation process associated with the rotation of ion pairs is also evident.[23,37] In some cases, this process dominates segmental relaxation to the extent that it is no longer visible. Because QENS is dominated by proton motion, ions contribute little to the signal, and we are able to isolate motion of the PEO spacer. Studies on ionomers using QENS have focused on the dynamics of the cation. Available studies include water dynamics and its influence on cation hopping and ion aggregation in Nafion[38−41] and the dynamics of hydrogen-rich cations in PTFE-based ionomers. In the latter case, the onset of cation mobility has been linked with the α-relaxation of the polymer.[42] In the current study, 95% of the hydrogen atoms are located on the polymer chains, and we observe segmental motion of the polymer.

Table 1. Ion Contents of Ionomers and PEO−Salt Samples

sample	cation:EO ratio	ion content	molecular weight (g/mol)
PEO600-0%Na	0	0	5800
PEO600-6%Na	1:217	0.005	5800
PEO600-11%Na	1:118	0.008	5800
PEO600-17%Na	1:76	0.013	8700
PEO600-49%Na	1:26	0.038	4700
PEO600-100%Na	1:13	0.077	6300
PEO/$LiClO_4$ 30:1	1:30	0.033	500000
PEO/$LiClO_4$ 14:1	1:14	0.071	500000
PEO/$LiClO_4$ 10:1	1:10	0.1	500000
PEO/$LiClO_4$ 8:1	1:8	0.125	500000
PEO/$LiClO_4$ 4:1	1:4	0.25	500000

We measure polymer mobility using QENS while varying the degree of sulfonation (*Y*%). We further establish a comparison to PEO/$LiClO_4$ systems based on previous work in our group.[28] The ion content of PEO salt systems is defined by the ether oxygen (EO) to Li ratio and falls in the range 4:1 to 50:1, although 8:1−14:1 are the most frequent targets because conductivity is maximized in this range. To connect the degree of sulfonation to this ratio, we consider the ion content, defined as the ratio of cations to ether oxygen atoms. This is the inverse of the ratio that is normally quoted, so that the nonionic polymer [0:1] has a well-defined value. Thus, in Table 1, we list the cation:EO ratios of the samples measured in this study. Ionomers with a PEO spacer of 600 MW are limited to ion contents of 0.077 (Na:EO = 1:13) or less, which is smaller than the range of ion contents normally studied in PEO/salt systems. The maximum conductivity of PEO600 ionomers occurs at an ion content of 0.013 (Na:EO = 1:76). This is both within the range we investigate and far lower than PEO/Li−salt systems; for example, the maximum conductivity of the PEO/ClO_4 system occurs at an ion content between 0.071 (Li:EO = 1:14) and 0.125 (Li:EO = 1:8). We consider the origin of this difference in the discussion section.

EXPERIMENTAL DETAILS

Sample Preparation. The ionomers were synthesized using poly(ethylene glycol) (PEG) oligomer diols and dimethyl 5-sulfoisophthalate sodium salt in a two-step melt transesterification process. The details of the preparation are established in a previous publication.[23] We used ^{1}H NMR to verify the molecular weight of the PEO spacers (600 g/mol in this study). We purified all ionomers by exhaustive diafiltration in deionized water to remove monomers, polymerization catalyst, and any ionic impurities. The concentrated ionomer solution was freeze-dried and then vacuum-dried at 120 °C to constant mass. To control the ion content, we vary the ratio of sulfonated (DMSSIS) and neutral (DMI) isophthalates. We label the resulting samples as PE600-*Y*%Na, where *Y* is the mole fraction of ionic isophthalate groups. The term "degree of sulfonation" refers to the percentage of isophthalate groups that are sulfonated.

Table 2. Relative Scattering Strength of Ionomer Components for PEO600-100%Na

	isophthalate + ions (%)	PEO spacer (%)	total (%)
coherent	1.39	5.15	6.54
incoherent	5.12	88.34	93.46
total	6.51	93.49	100.00

Neutron Scattering. We use quasi-elastic neutron scattering (QENS) to quantify polymer dynamics by monitoring the energy change of scattered neutrons. The scattering signal depends on the respective scattering cross sections of the constituent atoms: a quantitative measure of the probability of scattering. Among the atoms present in these ionomers (C, H, O, S, and Na) the scattering is dominated by incoherent scattering from hydrogen atoms. Since the majority of the hydrogen atoms are located on the PEO spacer (see Table 2), our measurements reflect the motion of this portion of the ionomer.

We conducted QENS measurements at the NIST Center for Neutron Research (NCNR) at the National Institute of Standards and Technology (NIST) in Gaithersburg, MD. To cover a larger dynamic range, we use two instruments: the disk chopper spectrometer (DCS)[43] and the high flux backscattering spectrometer (HFBS).[44] For the DCS, we operate at an incident wavelength of 4.8 Å, corresponding to an energy resolution of 56 μeV. This gives an upper bound on the time range at 50 ps. The lower bound on the time range, 0.4 ps, arises from interplay of the scattering vector and energy. The spatial scale accessible by the DCS in this configuration ranges from 3 to 11 Å. For the HFBS, we choose a dynamic range of $\pm$17 μeV (energy resolution of 0.85 μeV), corresponding to times between 250 and 2500 ps. The HFBS instrument geometry allows us to access a spatial scale of 4−11 Å. We obtained data for 298, 323, and 348 K allowing 1 h for thermal equilibration at each temperature.

Both instruments require an annular geometry for the sample. We prepare the sample as a uniformly thin ionomer film between aluminum foils. We calculate the film thickness to allow 10% of the neutrons to be scattered; this gives good signal intensity with low probability of multiple scattering. All sample data are measured against a resolution function obtained from a vanadium standard that is immobile at the conditions of the measurement. The intensity of scattered neutrons is a function of momentum transfer (Q) and frequency (ω). We reduce the raw data from the instrument using DAVE (Data Acquisition and Visualization Environment), an in-house software developed at the NCNR.[45] To give reduced data [$I(Q,\omega)$], DAVE uses the detector efficiencies obtained from the resolution data [$R(Q,\omega)$] and subtracts the background and the sample holder from the raw data.

The frequency domain data obtained from both the instruments are shown Figure 2. Data from the nonionic polymer [PEO600-0%Na] deviate more from the elastic resolution than that with 49% sulfonation [PEO600-49%Na], consistent with the idea that the presence of ions slows the polymer chain.

In order to effectively merge the data from the two instruments and allow for the possibility of using analytical fits with a stretched exponential, we inverse Fourier transform the data to the time domain. The total intensity $I(Q,\omega)$ is a convolution integral of the resolution function $R(Q,\omega)$ and sample dynamics $S(Q,\omega)$.

$$I(Q,\omega) = S(Q,\omega) \otimes R(Q,\omega) \quad (1)$$

In the time domain, $I(Q,t)$ is a product of the self-intermediate scattering function of the sample $S(Q,t)$ and resolution $R(Q,t)$.

$$I(Q,t) = S(Q,t)\cdot R(Q,t) \quad (2)$$

The self-intermediate scattering function, $S(Q,t)$, plotted in the time domain for both instruments in Figure 3 represents the correlation of

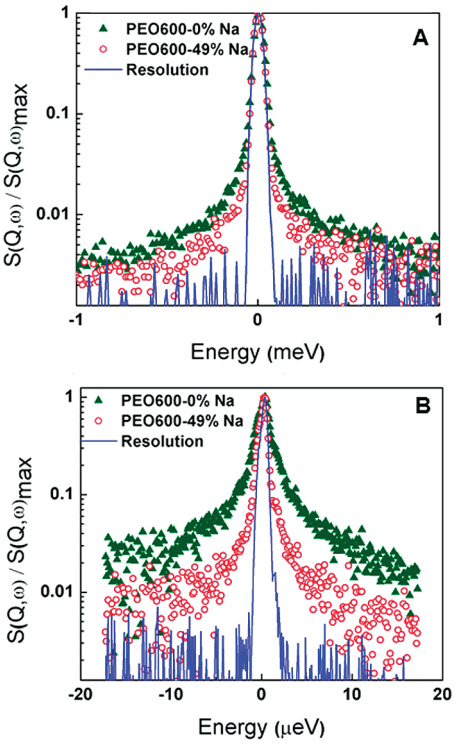

Figure 2. Frequency domain data from (A) DCS and (B) HFBS for PEO600-0% and PEO600-49%Na at Q = 1.04 Å^{-1}, T = 298 K.

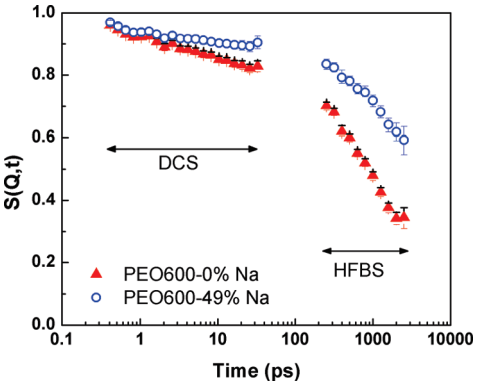

Figure 3. Inverse Fourier transformed data from DCS and HFBS for PEO600-0% and PEO600-49%Na at Q = 0.57 Å^{-1}.

atoms positions at time t relative to their positions at time zero. Note that the time points plotted do not exceed the instrumental resolution.

The data in Figure 3, as well as other $S(Q,t)$ data not shown, indicate that mobility of the PEO spacer reduces as we increase the ion content in the samples or lower the temperature, consistent with PEO-based SPEs in the amorphous phase.[1,28,35]

To describe the data in concise form, we fit the decays to obtain a characteristic relaxation time. For this purpose we recognize that the dynamics of polymers and other soft materials often exhibit a distribution of relaxation times, rather than Debye or single relaxation. Thus, we choose the stretched exponential or Kohlrausch−William−Watts[46] (KWW) expression

$$S(Q,t) = \exp\left[-\left(\frac{t}{\tau(Q)}\right)^{\beta(Q)}\right] \quad (3)$$

dx.doi.org/10.1021/ma2005074 |*Macromolecules* 2011, 44, 5381–5391

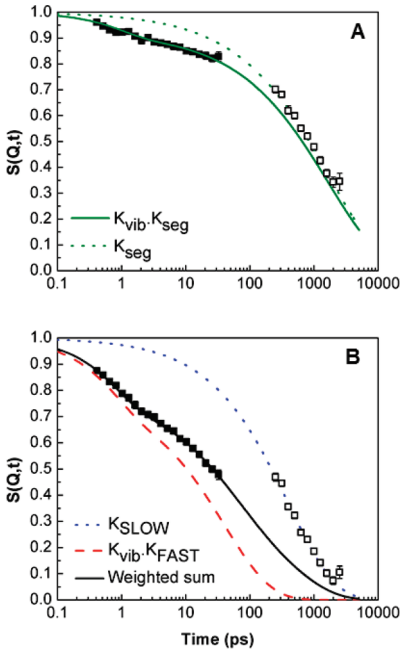

Figure 4. (A) Data for PEO600-0%Na at $Q = 1.04$ Å^{-1}, $T = 298$ K is fit to a single process K_{seg}. (B) Data for PEO600-17%Na at $Q = 1.04$ Å^{-1}, $T = 298$ K is fit to a weighted sum of two processes, K_{FAST} and K_{SLOW}.

where τ is the characteristic time and the stretching exponential β represents the width of the distribution.

Data Treatment. As with other polymers, amorphous PEO has a fast exponential decay that occurs on time scales of less than 2 ps, attributed to local cage vibrations and torsional librations.[47,48] Note that this decay is not prominent in Figure 3 due to the small Q value of that data. The simplest possible description of polymer motion over QENS time scales, and the one appropriate for pure PEO, is a fast exponential decay (K_{vib}) combined with the segmental relaxation K_{seg}:

$$S(Q,t) = K_{vib}K_{seg} \tag{4}$$

where

$$K_{vib} = \left(E_0(Q) + (1 - E_0(Q))\exp\left[-\left(\frac{t}{\tau_{vib}(Q)}\right)\right]\right) \tag{5}$$

and

$$K_{seg} = \exp\left[-\left(\frac{t}{\tau(Q)}\right)^{\beta(Q)}\right] \tag{6}$$

E_0 is the elastic incoherent structure factor for the vibration and represents the fraction of the decay allocated to segmental motion. Fast vibrations fall outside the HFBS window, and thus motion on this instrument reflects only K_{seg}. In Figure 4a, we have shown how a single process K_{seg} fits the data. This approach is successful for some cases, but not for some others (see Figure 4b), where a slower second process is required to describe the data from both instruments simultaneously. We cannot fit the data with a combined decay

$$K_{seg} = K_{FAST}K_{SLOW} \tag{7}$$

suggesting that all H atoms do not undergo both processes. Instead, a weighted sum

$$K_{seg} = X_{FAST}K_{FAST} + (1 - X_{FAST})K_{SLOW} \tag{8}$$

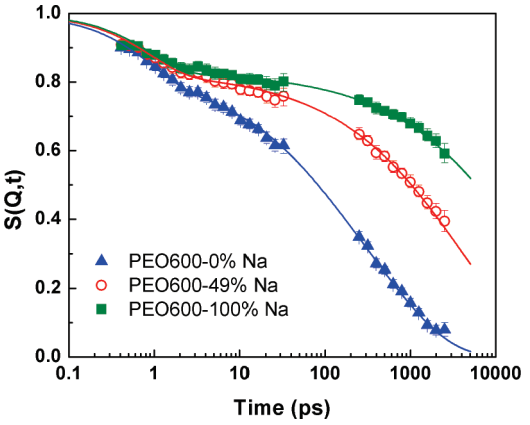

Figure 5. DCS data, shifted HFBS data, and the corresponding fitting lines for three samples at $T = 298$ K, $Q = 1.04$ Å^{-1}.

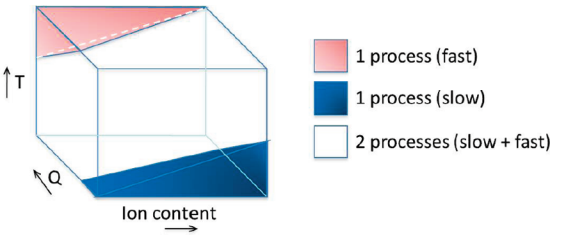

Figure 6. Occurrence of slow and fast processes as a function of ion content, Q, and temperature. The boundaries are approximate and are meant for visualization only.

is required, indicating that some H atoms belong to a "fast" subset (undergoing K_{FAST}) of the total H atoms and the rest belong to a "slower" subset (undergoing K_{SLOW}). In all the cases where two processes are observed, K_{FAST} has decayed to 0.2 or less before the HFBS window such that HFBS is only sensitive to K_{SLOW}.

To represent the data on a single plot, we shift the HFBS data such that K_{vib} and K_{FAST} are included in the decay. This is done by algebraic comparison of the full fit line (weighted sum in Figure 4) with only K_{SLOW} to determine the amount by which the data must be shifted. The resulting decay curve shows the data as if it was measured on a single instrument and does not affect the fitting algorithm, as shown in Figure 5.

There are two limiting cases where a single process is observed: high temperature and low ion content, in which only K_{FAST} is observed ($X_{FAST} \rightarrow 1$), and low temperature and high ion content, in which only K_{SLOW} is observed ($X_{FAST} \rightarrow 0$). Scenarios intermediate between these extremes require two processes to describe the data. This is presented pictorially in Figure 6 where the different shades show the identities and number of processes that constitute the dynamics.

The fitting is performed simultaneously on all data sets imposing the restrictions that relaxation times cannot increase with increasing temperature and Q, and τ_{FAST} should not exceed τ_{SLOW}. Because of the small time window of each instrument and the stretched nature of the relaxation, a range of fitting parameters can describe the data. We represent this range in the form of an error bar outside of which the parameter cannot represent the data, regardless of the values of the other parameters. To obtain the error bars, we generate 500 $S(Q,t)$ data sets within the instrument error. Each data set is fit using Levenberg–Marquardt nonlinear least-squares fitting program. To probe the entire parameter space, initial guesses for τ_{FAST} and τ_{SLOW} were randomized between 1 and 100 000 ps. We allowed β_{FAST} and β_{SLOW} to vary

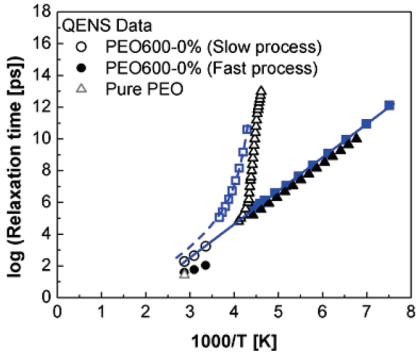

Figure 7. Temperature dependence of relaxation times obtained from QENS for PEO600-0%Na (circles), and for amorphous pure PEO (open gray triangle),[28] and DRS for PEO600-0%Na (squares),[23] and for pure PEO (black triangles).[66] For the DRS data, open symbols denote α-relaxation, and filled symbols denote β-relaxation. Error bars, if smaller than the data markers, are not shown.

between the limits of 0 and 1. X_{FAST} was held at the best fit value while calculating the range of fitting parameters. In the figures presented in this paper, we report mean ± [max, min] for the relaxation times.

RESULTS AND DISCUSSION

Dynamics in the Nonionic Polymer. We first compare QENS data to other available probes of segmental motion for the nonionic polymer, in this case broadband dielectric relaxation spectroscopy (DRS). In Figure 7 we compare the two processes obtained from QENS with DRS[23] data. The DRS experiment measures the reorientation of local dipoles and is not spatially resolved. The lowest Q values in QENS data typically provide the best comparison. For pure PEO, it has been noted that Q = 1.02 Å^{-1} or higher is more segmental in nature than Q = 1.51 Å^{-1}.[65] For this comparison, we chose Q = 0.57 Å^{-1} for the slow process and Q = 0.89 Å^{-1} for the fast process because this process is not present at Q = 0.57 Å^{-1}. Note that the difference between the fast and slow processes is larger than differences due to spatial scale. The DRS data includes the α-relaxation corresponding to segmental motion and a β-relaxation attributed to local chain twisting in the PEO spacers.[23] As with other studies, the QENS data represent the merged α/β-relaxation evident at temperatures greater than 1.3T_g.[49] Our slow process data are consistent with DRS measurements on the nonionic polymer. The fast process more closely resembles the merged α/β process of pure PEO, also shown in Figure 7. Although the β-relaxations in pure PEO and the nonionic polymer [the difference being the presence of the isophthalate comonomer] are nearly coincident, the β-relaxation can change slope after merging with the α-relaxation.[67] It is not known if this occurs in pure PEO; however, QENS data on pure PEO are consistent with the times obtained for the fast process. The fast process does not appear to coincide with the β-relaxation of the ionomer. We conclude that the QENS data are consistent with reported measures of segmental mobility in the nonionic polymer, with the slow process resembling the ionomer and the fast process resembling pure PEO.

We determine the influence of the isophthalate monomer on PEO dynamics by comparing the nonionic polymer to pure PEO. Pure PEO is amorphous at 348 K and undergoes one segmental relaxation.[28,50,51] Segmental relaxation in polymers depends on

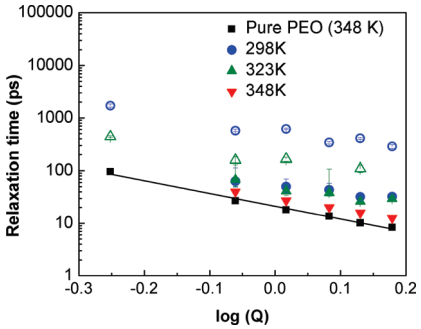

Figure 8. Relaxation times from K_{FAST} (filled symbols) and K_{SLOW} (open symbols) for the nonionic polymer. Data for pure PEO are at 343 K. The units of Q are in Å^{-1}.

Q via $\tau \sim Q^{-n}$ where n varies from −2 to −2/β.[50−52] As shown in Figure 8, both K_{FAST} and K_{SLOW} are segmental processes with the same slope as pure PEO. At 348 K, only the faster relaxation (K_{FAST}) is present in the nonionic polymer; it is slowed slightly compared to pure PEO. This slowing reflects the influence of the isophthalate group on segmental relaxation of the PEO spacer. At lower temperatures (298 and 323 K), we observe the slower, second process (K_{SLOW}) that is also a segmental relaxation.

One possible explanation for two classes of segmental motion is the proximity of the atoms to the comonomer: H atoms near the isophthalate group may be slower than those in the midsegment. In a previous study of disordered diblock copolymers of PEO and PMMA,[53] we determined that mobility of the fast PEO block (T_g = 221 K) is significantly slowed by covalent bonding to the slow PMMA block (T_g = 391 K) for 5−6 backbone atoms adjacent to the bond. This is not observed experimentally in the case of high molecular weight diblocks because the number of atoms influenced by the bond is a small fraction of the total. This is not the case for the PEO 600 ionomer, in which the spacer has 13 repeat units with 39 backbone atoms. If this system behaves as the PEO/PMMA simulation, a reasonable fraction (∼30%) of the backbone atoms in the PEO spacer would be slowed by direct connection to the isophthalate group. This depends on the isophthalate group being "slow" compared to PEO, a reasonable assumption since PEO has a T_g of 220 K and polymers with repeat units similar to isophthalate have high T_g (e.g., the T_g of polyethylene terephthalate is 343 K). Thus, the mobility of the PEO spacer might be influenced by the isophthalate group in a significant enough fraction that it is observed in our experiments. Preliminary results from molecular dynamics simulations on PEO600-100%Na show this behavior: displacements of hydrogen atoms over time intervals of 2−10 ns are smallest near the isophthalate group and reach a maximum at the chain midpoint.[54] From these observations, we suggest that the "fast" motion (K_{FAST}) corresponds to the midregion hydrogen atoms and the "slow" motion (K_{SLOW}) represents hydrogen atoms close to the isophthalate comonomer. This is illustrated in Figure 9, where we introduce the terms "bridge atoms" and "anchor atoms" to describe the fast and slow fractions. This terminology is used throughout the remainder of the paper. We remind the reader that although the presence of two dynamic processes is an experimental observation, the classification as bridge and anchor atoms is our interpretation of this observation.

The interpretation presented above divides mobility of the PEO H atoms into two classes: bridge atoms [segmental and similar to pure PEO] and anchor atoms [significantly slower but

dx.doi.org/10.1021/ma2005074 |Macromolecules 2011, 44, 5381–5391

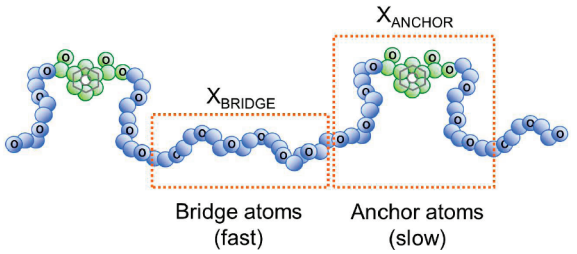

Figure 9. Illustration of the spatial location of fast and slow portions of the nonionic polymer.

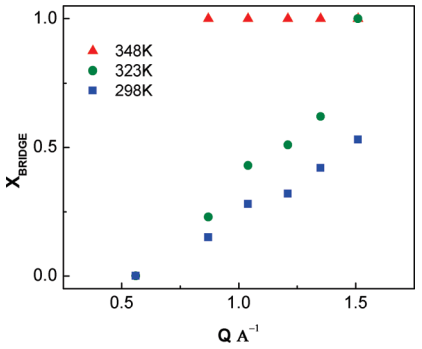

Figure 10. Fraction of bridge atoms in the nonionic polymer as a function of Q.

still segmental]. The fraction X_{BRIDGE} denotes the fraction of bridge atoms and is given in Figure 10 for the nonionic polymer. It may appear counterintuitive that the fraction of bridge atoms depends on spatial scale. To understand this observation, we must consider the physical meaning of the spatial scale of the measurements. To a first approximation, the spatial scale Q sets the radius of a sphere centered at each atom, and ask about movement within this sphere: when the atom leaves the sphere, its $S(Q,t)$ falls to zero. At low Q values that correspond to large radii of observation (~11 Å), all atoms appear to be influenced by the isophthalate group (X_{BRIDGE} = 0). This is because the observation volume encompasses the entire PEO spacer (R_g ~ 9 Å for 13 repeat units[55]), and motion on this scale is controlled by the slowest anchor atoms. As we decrease the size of observation radius, the contribution of bridge atoms becomes more prominent and X_{BRIDGE} increases.

Only a single process is observed at T = 348 K, consistent with bridge atoms. Dynamics of the slower anchor atoms only become distinct when the temperature is lowered. For two processes to be observed, the average relaxation times of anchor atoms must be significantly greater than bridge atoms, and the variation must be sharply divided; otherwise, a single relaxation with low β would fit the data. The emergence of two processes as temperature is lowered occurs because the PEO spacer and the more rigid isophthalate group likely have different temperature dependencies. At high temperature, the difference in dynamics between bridge and anchor atoms is not sufficient to resolve into two processes, but as temperature is lowered, anchor atoms slow more than their faster bridge counterparts. This leads to increasing differences between bridge and end segments and the eventual emergence of two processes. In Figure 11, we show the increasing difference between bridge and anchor atom relaxation times as temperature decreases.

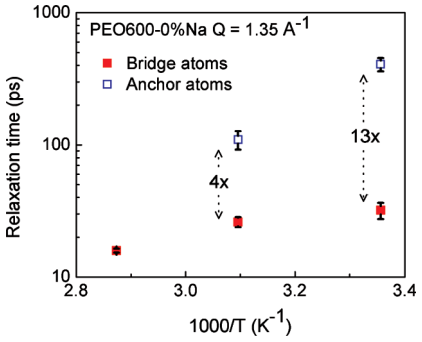

Figure 11. Comparison of the temperature dependencies of bridge and anchor atoms in the nonionic polymer.

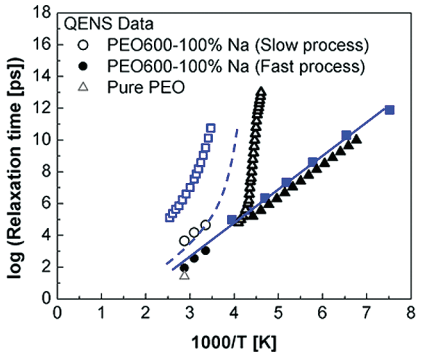

Figure 12. Temperature dependence of relaxation times obtained from QENS for PEO600-100%Na (circles), and for amorphous pure PEO (open gray triangle),[28] and DRS for PEO600-100%Na (squares),[23] and for pure PEO (black triangles).[66] For the DRS data, open symbols denote α-relaxation, and filled symbols denote β-relaxation. The dashed line corresponds to the α-relaxation of the nonionic polymer as seen from DRS (Figure 7). Error bars, if smaller than the data marker, have not been shown.

Effect of Ion Content on Ionomer Dynamics. In the previous section we identified two segmental relaxation processes associated with the PEO hydrogen atoms in the nonionic polymer: bridge atoms in the spacer midregion and anchor atoms neighboring the isophthalate group. In this section we discuss the effects of ion content on both relaxations.

In Figure 12, we compare relaxation times obtained via QENS with dielectric times for the PEO600-100%Na sample. Spatial scales are selected as described for Figure 7. Two processes are evident in the DRS data: the β-relaxation at low temperature and a slower relaxation, the origin of which is discussed below. Unlike the nonionic polymer, the end atom QENS data do not appear to represent the merger of the two DRS relaxations, but rather the continuation of the β-relaxation. In DRS measurements of the Li analogue of this sample, PEO600-100%Li, the local β-relaxation, the segmental α-relaxation, and a new process [termed α_2] are evident.[23] The α_2-relaxation process follows the temperature dependence of the segmental relaxation, is 2 orders of magnitude slower, and is interpreted as the reorientation of dipoles formed by ion pairs. When the ion is changed to sodium, only one process is clearly resolvable,[56] and its time scale more closely follows the α_2-relaxation. This behavior is consistent with the aggregation behavior of the system as observed via SAXS: in PEO600-100%Li, ionic aggregation is

dx.doi.org/10.1021/ma2005074 |Macromolecules 2011, 44, 5381–5391

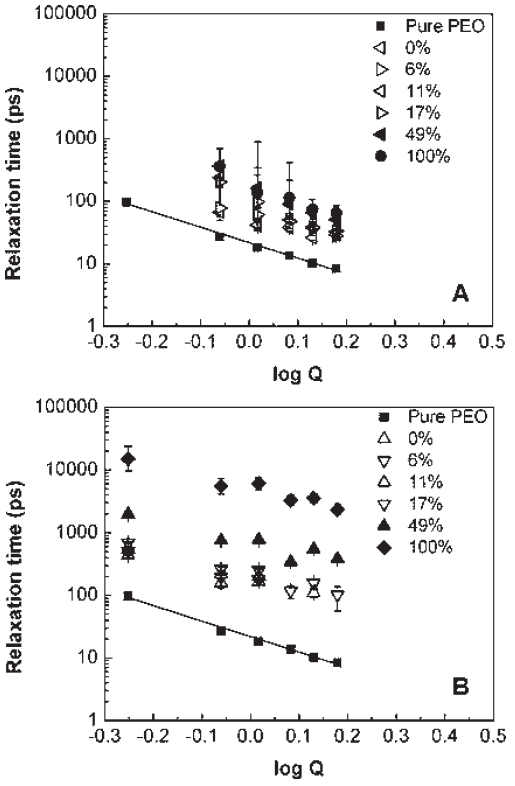

Figure 13. Q dependence of the relaxation times for the ionomers at 298 K for (A) bridge atoms and (B) anchor atoms. The single relaxation for pure PEO is shown in both parts of the figure. The solid line through pure PEO data represents $\tau \sim Q^n$ where $n = -2.48$.[28] The units of Q are in $Å^{-1}$.

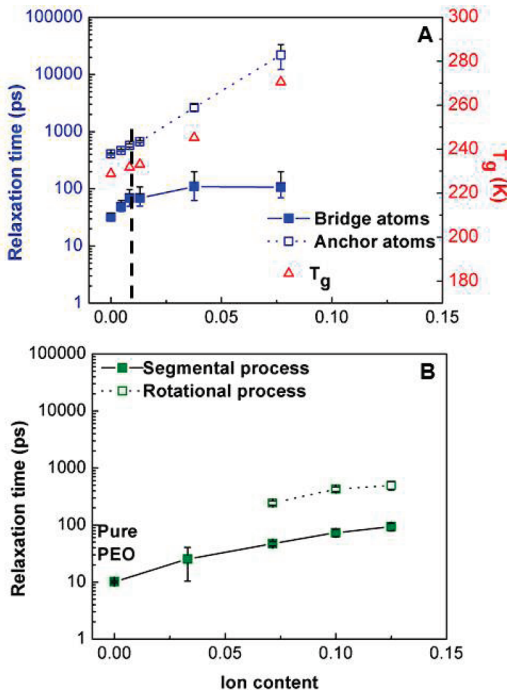

Figure 14. (A) Relaxation times for PEO600-*Y*%Na ionomers [298 K, $Q = 1.35$ $Å^{-1}$] and T_g vs ion content (B) relaxation times for PEO/$LiClO_4$ [348 K, $Q = 1.35$ $Å^{-1}$] and T_g vs ion content.[28]

observed at all temperatures, whereas for PEO600-100%Na, well-defined ionic aggregates form upon increasing temperatures from 298 to 393 K. This emerges to a lesser extent and only at temperatures above our measurements.[21,57] Apparently, the better dispersion of ions in PEO600-100%Na causes the contribution from ion pairs to overshadow the PEO segmental process to the extent that it is no longer clearly resolvable using DRS. QENS, which does not observe ion or dipole motion, is still able to resolve the segmental relaxation in this sample.

As illustrated in Figure 13, the presence of ions does not give rise to any new processes, nor does it change the physical origins of the two processes observed in the nonionic polymer. Both processes remain segmental in nature with ion addition, as shown by the Q dependence of relaxation times. It is clear from Figure 13 that increasing the ion content has different effects on the dynamics of the two processes.

In Figure 14A we plot relaxation times at $Q = 1.35$ $Å^{-1}$ as a function of ion content. While the relaxation times of bridge atoms increase by a small amount ($\tau_{BRIDGE,100\%}/\tau_{BRIDGE,0\%} \sim 3$), those of anchor atoms increase significantly ($\tau_{END,100\%}/\tau_{END,0\%} \sim 50$). An ion content of 0.01 divides two regimes with different behavior. In the first regime [ion contents <0.01], bridge relaxation times vary, whereas end relaxation times are relatively constant. DRS relaxation times for the PEO600-Li series are insensitive to ion content up to the same value.[23] This suggests that the segmental process, when observable with DRS, better corresponds to anchor atoms, as opposed to bridge atoms. In the second regime [ion contents >0.01], the trend reverses: relaxation times of bridge atoms are relatively constant, whereas those of anchor atoms increase substantially.

On the basis of these observations and the idea that relaxation times slow when ion content increases, we suggest the following scenario. Ions initially populate the bridge segments. As concentration increases past 0.01 [118 EO per cation], ions populate the end segments. In the extreme case that no further ions populated bridge regions, there would be 1 cation for 118 total EO in the PEO600-100%Na sample. If we consider the fraction of bridge atoms as 25% (a representative value from Figure 10 at 298 K), there would be one cation for 30 bridge EOs, or a bridge atom concentration of 30 EO per cation. Since the entire PEO spacer is 13 EO, there are 3.25 bridge EOs per spacer, meaning that bridge atoms from (30/3.25 ~) 9 PEO spacers share 1 cation. The anchor atoms from these 9 spacers ($9 \times 9.75 \sim 88$ EO atoms) share the remaining 8 cations. This yields an anchor atom ion content of 11 EO per cation. This rough estimate implies that 1 out of every 9 cations is "single" (no association with its anion), whereas the other 8 participate in shared ion pairs, separated ion pairs, or larger aggregates.

The behavior of the PEO salt system PEO/$LiClO_4$ with ion content is presented in Figure 14b for comparison. In this system, the presence of ions slows down the segmental relaxation process by electrostatic coordination between the cation and the ether-oxygen atoms of the PEO chain. The influence of ion content on segmental relaxation times is similar to that of the bridge atoms in the ionomer: between 0.025 and 0.12, the relaxation time increases by a factor of 3. However, the variation is continuous, rather than divided into two regimes. In contrast, the slower processes have distinctly different trends, confirming that the origins of these processes are different. Indeed, the slower process in PEO/$LiClO_4$ is rotational in nature and unrelated to the slower process in the ionomer. PEO/Li−salt systems

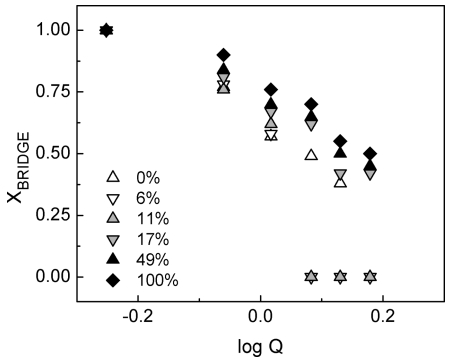

Figure 15. Fractions of slow H atoms, X_{ANCHOR}, as a function of Q for all samples at T = 323 K. The legend entries "Y%" correspond to PEO600-Y%Na. Darker data points have higher ion content than lighter data points. The units of Q are in $Å^{-1}$.

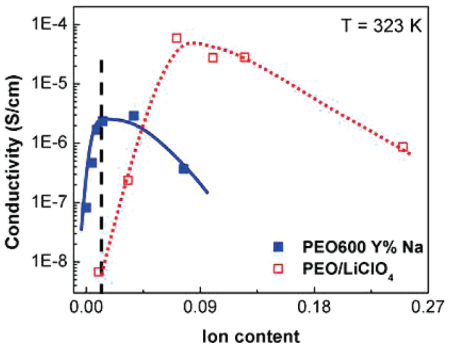

Figure 16. Conductivity vs ion content for the PEO600-Y%Na ionomers[56] and PEO/$LiClO_4$[28] at T = 348 K. The curves through these data points serve as visual aids to identify the conductivity peaks.

crystallize into pure PEO and ion-containing structures with EO:Li ratios of 3:1 or 6:1, depending on the electrolyte concentration.[32,33,58] It is the rotation of these structures that defines the slower process. These structures do not exist in the ionomers, as WAXS studies on the PEO600-based ionomers do not show the formation of crystalline structures in the temperature range of measurement.[21,22] Although it is possible that small helical structures exist locally, our results are not consistent with a rotation, for which relaxation times are Q independent.[28]

The increase in relaxation times of anchor atoms exceeds that which is expected from electrostatic coordination of the cation with the PEO spacer. Although the maximum ion content of the ionomers is 0.08, we estimate that for the anchor atoms the concentration may be as high as 11 EO per cation [0.14]. The relaxation times of anchor atoms increase by a factor of 50 over this range, whereas relaxation times of PEO/$LiClO_4$ vary by a factor of 9. This suggests that something other than electrostatic coordination via cations and ether oxygens influences dynamics in the anchor atom region. In the PEO/Li−salt system, ion pairs or larger aggregates do not involve the polymer chain. This is not the case for the ionomer. Interaction between at least two anions and a cation can form physical cross-links via ionic clusters, which do not occur in PEO/Li−salt systems. We know that these clusters are not well-defined, large, or of consistent size because ionic aggregation is not evident in the SAXS data for PEO600-100%Na below 353 K.[21,57] However, it is reasonable to assume small, polydisperse clusters with weak boundaries are present in PEO600-100%Na, based on the excess scattering intensity in the SAXS data between the interchain packing peak (amorphous halo) and the ionomer peak evident in the PEO600-100% Li ionomer. This provides a mechanism for slowing in excess of the PEO/Li salt case: ionic cross-linking preferentially slows the chain near the anions, leaving the bridge region unaffected. We also note that X_{ANCHOR} increases with ion content (see Figure 15). This could occur if more ether oxygens associate with small ionic clusters.

The glass transition temperature increases with ion content from 229 K for the nonionic polymer to 271 K for PEO600-100% Na. This is compared to the ion content dependence of bridge and end relaxation times in Figure 14. It is clear that the anchor atoms control T_g, rather than the bridge atoms. The reason for this is similar to the reason only the slow process is observed at the largest length scales of our experiments. In the concept of the cooperatively rearranging region, the length scale associated with T_g is ∼100 Å.[59] A region of this size would include multiple PEO spacers and their associated ions, and thus we expect it to encompass multiple dynamic processes. The dynamics of the region will be controlled by the slowest of those processes.

In PEO/salt systems, it is established that the segmental motion of the polymer facilitates ion motion. Conductivity depends on both the mobility of the host polymer and the ion content. Since increasing ion content both provides more ions for conduction and slows polymer mobility, a peak is observed in conductivity. As shown in Figure 16, a peak also occurs in the ionomers. The maximum conductivity occurs at lower ion content in the ionomers than in PEO/$LiClO_4$. This is directly related to the positioning of the anion on the polymer backbone and its influence on polymer mobility. In the ionomers, cations slow the polymer in two ways: coordination with ether oxygen atoms in bridge regions and ionic cross-linking in end regions. The latter is absent in PEO/$LiClO_4$, as the anion is not bonded to the PEO chain, and thus salt clusters do not cross-link the polymer. As a result, only interaction with PEO ether oxygen atoms (comparable to the bridge region) slows polymer mobility in PEO/salt systems. Because of this difference, higher ion content may be tolerated in PEO/salt systems before sluggish polymer dynamics decreases conductivity. The rapid rise of conductivity for the ionomers and the positioning of optimal conductivity at low ion content may be important in designing low ion content electrolytes. We note, however, that the conductivities of these two samples should not be directly compared. The ionomers are essentially single ion conductors, whereas in PEO/$LiClO_4$ both the anions and the cations contribute to conductivity. The identity of the anion is also different, which has been demonstrated to influence conductivity.[60,61]

We conclude by discussing several structures that may be important and their importance in our data and other measurements on PEO600-100%Na. Figure 17 proposes four such structures: the single cation, the separated contact pair, the shared contact pair, and a small ionic aggregate. We emphasize that our measurements do not directly reveal these structures, and their connection with our data is our interpretation. Single cations (also sometimes called "free" ions) are solvated by PEO ether oxygens and have limited interaction with anions. The ions interacting with bridge ether oxygens are most likely single cations. Although we estimate no more than 7% single ions, an FTIR study indicates that all of the SO_3 groups are associated with a cation (direct contact pairs or aggregates), with no detectable single cations.[25] In molecular simulations, close to 30% of

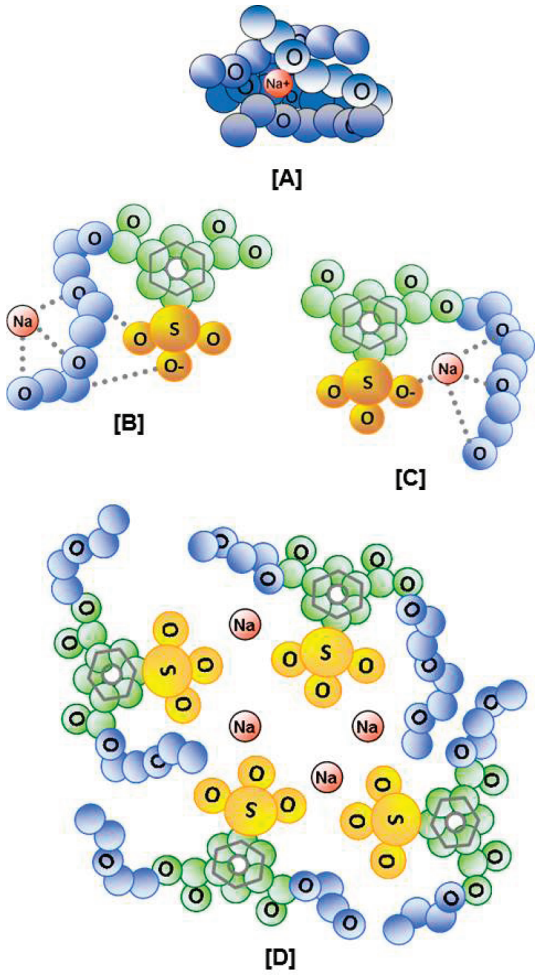

Figure 17. Cation coordination states (A) single cation, (B) separated contact pair, (C) shared contact pair, and (D) small ionic aggregate.

Na are found as single cations, and 20% are in direct contact pairs.[54] The separated contact pair, in which a PEO segment lies between the anion and cation, occurs regularly in PEO/Li salt systems; this can be classified as free or as a pair, depending on technique. This structure is found in simulation,[54] and there is some evidence it may be present based on DRS.[23] The current data do not require or exclude such structures. Indeed, the techniques used to date (SAXS,[21,57] molecular simulation,[54] DRS,[23,56] and QENS) suggest that at the temperatures of our measurements a variety of structures are present in PEO600-100%Na. One structure that appears consistent with all techniques used to date and is also consistent with previous observations on ion containing polymers[7,62−64] is the small ionic aggregate. The current measurements suggest that small ionic clusters lead to ionic cross-links, slowing polymer dynamics in excess of what is expected based on PEO−salt systems. Ionic aggregates are not evident in SAXS in PEO600-100%Na at room temperature,[57] indicating that the clusters are small and inconsistent in size. Ionic aggregates become evident via SAXS in PEO600-100%Na above 353 K. In molecular simulations, 50% of Na ions cluster in ionic aggregates of 3−12 ions.[54] Aggregates are also seen in DRS, with their fraction increasing with temperature.[57] It appears that these aggregates are characteristic of PEO-based single ion conductors, and their size and regularity depend on ion identity and temperature.[57] The influence of ion identity on polymer structures has been reported,[21,57] and the polymer dynamics using QENS will be the subject of a future publication.

CONCLUDING REMARKS

In this study we used QENS to measure dynamics in PEO-based single ion conductors of the form PEO600-*Y*%Na where *Y* = [0,100]. The presence of the isophthalate group in the nonionic polymers slows segmental relaxation seen in pure PEO and introduces an additional segmental relaxation that is slower. Our interpretation associates these relaxations with segments in the midregion of the repeating unit [bridge atoms] and segments neighboring the isophthalate group [anchor atoms]. Ionomers with nonzero ion content also show two segmental relaxations. The presence of ions does not change the origins of the two processes, but does slow them down. The anchor atoms slow significantly more than the bridge atoms as ion content increases. We suggest this is due to the presence of small ionic clusters, which cross-link the polymer chains. These cross-links are either more stable or more extensive than those formed between bridge ether oxygens and cations, as the influence of ion content on anchor atom dynamics is stronger than in PEO−salt systems.

AUTHOR INFORMATION

Corresponding Author
*E-mail: jmaranas@psu.edu.

ACKNOWLEDGMENT

This work is supported by the Department of Energy, Office of Basic Energy Sciences, under Grant DEFG02-07ER46409. The authors gratefully acknowledge Shichen Dou for ionomer synthesis and Greg Tudryn for dialysis. We also thank Ralph Colby, Jim Runt, Karl Mueller, and Karen Winey for helpful discussions. This work utilized facilities supported in part by the National Science Foundation under Agreement DMR-0454672. We acknowledge the support of the National Institute of Standards and Technology, U.S. Department of Commerce, in providing the neutron research facilities used in this work.

REFERENCES

(1) Mao, G. M.; Perea, R. F.; Howells, W. S.; Price, D. L.; Saboungi, M. L. Relaxation in polymer electrolytes on the nanosecond timescale. *Nature* **2000**, *405* (6783), 163–165.

(2) Triolo, A.; Arrighi, V.; Triolo, R.; Passerini, S.; Mastragostino, M.; Lechner, R. E.; Ferguson, R.; Borodin, O.; Smith, G. D. Dynamic heterogeneity in polymer electrolytes. Comparison between QENS data and MD simulations. *Physica B* **2001**, *301* (1−2), 163–167.

(3) Borodin, O.; Smith, G. D. Molecular dynamics simulations of poly(ethylene oxide)/LiI melts. 2. Dynamic properties. *Macromolecules* **2000**, *33* (6), 2273–2283.

(4) Ouyang, C. Y.; Shi, S. Q.; Wang, Z. X.; Huang, X. J.; Chen, L. Q. First-principles study of Li ion diffusion in $LiFePO_4$. *Phys. Rev. B* **2004**, *69*, 10.

(5) Gray, F. M. *Polymer Electrolytes*; The Royal Society of Chemistry: Letchworth, UK, 1997.

(6) Xu, K. Nonaqueous liquid electrolytes for lithium-based rechargeable batteries. *Chem. Rev.* **2004**, *104* (10), 4303–4417.

(7) Hamaide, T.; Ledeore, C. Cationic Conductivity and Relaxation Processes in Solid Polymer Electrolytes with Lithium Perfluoroalkyl

Sulfonate or Sulfonato End-Capped Poly(Ethylene Oxide). *Polymer* **1993**, *34* (5), 1038–1046.

(8) Rawsky, G. C.; Fujinami, T.; Shriver, D. F. Aluminosilicate Poly(Ethylene Glycol) Copolymers - a New Class of Polyelectrolytes. *Chem. Mater.* **1994**, *6* (12), 2208–2209.

(9) Sun, X.-G.; Kerr, J. B. Synthesis and Characterization of Network Single Ion Conductors Based on Comb-Branched Polyepoxide Ethers and Lithium Bis(allylmalonato)borate. *Macromolecules* **2005**, *39* (1), 362–372.

(10) Sun, X.-G.; Kerr, J. B.; Reeder, C. L.; Liu, G.; Han, Y. Network Single Ion Conductors Based on Comb-Branched Polyepoxide Ethers and Lithium Bis(allylmalonato)borate. *Macromolecules* **2004**, *37* (14), 5133–5135.

(11) Ito, K.; Ohno, H. Ionic conductivity of poly(ethylene oxide) having charges on the chain end. *Solid State Ionics* **1995**, *79*, 300–305.

(12) Bronstein, L. M.; Karlinsey, R. L.; Stein, B.; Yi, Z.; Carini, J.; Zwanziger, J. W. Solid polymer single-ion conductors: Synthesis and properties. *Chem. Mater.* **2006**, *18* (3), 708–715.

(13) Ito, K.; Ohno, H. Ionic-Conductivity of Poly(Ethylene Oxide) Having Charges on the Chain-End. *Solid State Ionics* **1995**, *79*, 300–305.

(14) Ito, K.; Nishina, N.; Tominaga, Y.; Ohno, H. Effect of terminal groups on the ionic conductivity of alpha,omega-dicharged poly(ethylene oxide) oligomers. *Solid State Ionics* **1996**, *86−8*, 325–328.

(15) Zhou, G.; Khan, I.; Smid, J. Solvent-free cation-conducting polysiloxane electrolytes with pendant oligo(oxyethylene) and sulfonate groups. *Macromolecules* **1993**, *26* (9), 2202–2208.

(16) Ohno, H.; Kobayashi, N.; Takeoka, S.; Ishizaka, H.; Tsuchida, E. Larger cations can move faster in solid polymer electrolytes. *Solid State Ionics* **1990**, *40−41* (Part 2), 655–658.

(17) Tsuchida, E.; Ohno, H.; Kobayashi, N.; Ishizaka, H. Poly[(Î¹-carboxy)oligo(oxyethylene) methacrylate] as a new type of polymeric solid electrolyte for alkali-metal ion transport. *Macromolecules* **1989**, *22* (4), 1771–1775.

(18) Klein, R. J.; Runt, J. Plasticized single-ion polymer conductors: Conductivity, local and segmental dynamics, and interaction parameters. *J. Phys. Chem. B* **2007**, *111* (46), 13188–13193.

(19) Doeff, M. M.; Reed, J. S. Li ion conductors based on laponite/poly(ethylene oxide) composites. *Solid State Ionics* **1998**, *113*, 109–115.

(20) Kobayashi, N.; Uchiyama, M.; Tsuchida, E. Poly[lithium methacrylate-co-oligo(oxyethylene)methacrylate] as a solid electrolyte with high ionic conductivity. *Solid State Ionics* **1985**, *17* (4), 307–311.

(21) Wang, W. Q.; Liu, W. J.; Tudryn, G. J.; Colby, R. H.; Winey, K. I. Multi-Length Scale Morphology of Poly(ethylene oxide)-Based Sulfonate Ionomers with Alkali Cations at Room Temperature. *Macromolecules* **2010**, *43* (9), 4223–4229.

(22) Dou, S. C.; Zhang, S. H.; Klein, R. J.; Runt, J.; Colby, R. H. Synthesis and characterization of poly(ethylene glycol)-based single-ion conductors. *Chem. Mater.* **2006**, *18* (18), 4288–4295.

(23) Fragiadakis, D.; Dou, S.; Colby, R. H.; Runt, J. Molecular mobility and Li+ conduction in polyester copolymer ionomers based on poly(ethylene oxide). *J. Chem. Phys.* **2009**, *130*, 6.

(24) Fragiadakis, D.; Dou, S. C.; Colby, R. H.; Runt, J. Molecular mobility, ion mobility, and mobile ion concentration in poly(ethylene oxide)-based polyurethane ionomers. *Macromolecules* **2008**, *41* (15), 5723–5728.

(25) Lu, M. F.; Runt, J.; Painter, P. An Infrared Spectrocopic Study of a Polyester Copolymer Ionomer Based on Poly(ethylene oxide). *Macromolecules* **2009**, *42* (17), 6581–6587.

(26) Carlsson, P.; Zorn, R.; Andersson, D.; Farago, B.; Howells, W. S.; Borjesson, L. The segmental dynamics of a polymer electrolyte investigated by coherent quasielastic neutron scattering. *J. Chem. Phys.* **2001**, *114* (21), 9645–9656.

(27) Mos, B.; Verkerk, P.; Pouget, S.; van Zon, A.; Bel, G. J.; de Leeuw, S. W.; Eisenbach, C. D. The dynamics in polyethylene-oxide-alkali iodide complexes investigated by neutron spin-echo spectroscopy and molecular dynamics simulations. *J. Chem. Phys.* **2000**, *113* (1), 4–7.

(28) Fullerton-Shirey, S. K.; Maranas, J. K. Effect of LiClO4 on the Structure and Mobility of PEO-Based Solid Polymer Electrolytes. *Macromolecules* **2009**, *42* (6), 2142–2156.

(29) Mao, G.; Saboungi, M. L.; Price, D. L.; Badyal, Y. S.; Fischer, H. E. Lithium environment in PEO-LiClO4 polymer electrolyte. *Europhys. Lett.* **2001**, *54* (3), 347–353.

(30) Triolo, A.; Lo Celso, F.; Passerini, S.; Arrighi, V.; Lechner, R. E.; Frick, B.; Triolo, R. Segmental dynamics in polymer electrolytes. *Appl. Phys. A: Mater. Sci. Process.* **2002**, *74* (0), s493–s495.

(31) Mao, G. M.; Saboungi, M. L.; Price, D. L.; Armand, M. B.; Howells, W. S. Structure of liquid PEO-LiTFSI electrolyte. *Phys. Rev. Lett.* **2000**, *84* (24), 5536–5539.

(32) Robitaille, C. D.; Fauteux, D. Phase-Diagrams and Conductivity Characterization of Some Peo-Lix Electrolytes. *J. Electrochem. Soc.* **1986**, *133* (2), 315–325.

(33) Edman, L.; Ferry, A.; Doeff, M. M. Slow recrystallization in the polymer electrolyte system poly(ethylene oxide)(n)-LiN(CF3SO2)(2). *J. Mater. Res.* **2000**, *15* (9), 1950–1954.

(34) Maranas, J. K. Solid Polymer Electrolytes. In *Dynamics of Soft Matter: Neutron Applications*; Springer, in press.

(35) Mao, G. M.; Saboungi, M. L.; Price, D. L.; Armand, M.; Mezei, F.; Pouget, S. alpha-relaxation in PEO-LiTFSI polymer electrolytes. *Macromolecules* **2002**, *35* (2), 415–419.

(36) Londono, J. D.; Annis, B. K.; Habenschuss, A.; Borodin, O.; Smith, G. D.; Turner, J. Z.; Soper, A. K. Cation Environment in Molten Lithium Iodide Doped Poly(ethylene oxide). *Macromolecules* **1997**, *30* (23), 7151–7157.

(37) Zhang, S. H.; Dou, S. C.; Colby, R. H.; Runt, J. Glass transition and ionic conduction in plasticized and doped ionomers. *J. Non-Cryst. Solids* **2005**, *351* (33−36), 2825–2830.

(38) De Luca, E.; Waigh, T. A.; Monkenbusch, M.; Kim, J. S.; Jeon, H. S. Neutron spin echo study of the dynamics of micellar solutions of randomly sulphonated polystyrene. *Polymer* **2007**, *48* (14), 3930–3934.

(39) Paciaroni, A.; Casciola, M.; Cornicchi, E.; Marconi, M.; Onori, G.; Pica, M.; Narducci, R. Temperature-dependent dynamics of water confined in Nafion membranes. *J. Phys. Chem. B* **2006**, *110* (28), 13769–13776.

(40) Perrin, J. C.; Lyonnard, S.; Volino, F. Quasielastic neutron scattering study of water dynamics in hydrated nafion membranes. *J. Phys. Chem. C* **2007**, *111* (8), 3393–3404.

(41) Pivovar, A. A.; Pivovar, B. S. Dynamic behavior of water within a polymer electrolyte fuel cell membrane at low hydration levels. *J. Phys. Chem. B* **2005**, *109* (2), 785–793.

(42) Page, K. A.; Park, J. K.; Moore, R. B.; Sakai, V. G. Direct Analysis of the Ion-Hopping Process Associated with the alpha-Relaxation in Perfluorosulfonate Ionomers Using Quasielastic Neutron Scattering. *Macromolecules* **2009**, *42* (7), 2729–2736.

(43) Copley, J. R. D.; Cook, J. C. The Disk Chopper Spectrometer at NIST: a new instrument for quasielastic neutron scattering studies. *Chem. Phys.* **2003**, *292* (2−3), 477–485.

(44) Meyer, A.; Dimeo, R. M.; Gehring, P. M.; Neumann, D. A. The high-flux backscattering spectrometer at the NIST Center for Neutron Research. *Rev. Sci. Instrum.* **2003**, *74* (5), 2759–2777.

(45) Azuah, R. T.; Kneller, L. R.; Qiu, Y.; Tregenna-Piggott, P. L. W.; Brown, C. M.; Copley, J. R. D.; Dimeo, R. M. DAVE: A comprehensive software suite for the reduction, visualization, and analysis of low energy neutron spectroscopic data. *J. Res. Natl. Inst. Stand. Technol* **2009**, *114* (6), 341–358.

(46) Williams, G.; Watts, D. C. Non-Symmetrical Dielectric Relaxation Behaviour Arising from a Simple Empirical Decay Function. *Trans. Faraday Soc.* **1970**, *66* (565P), 80–&.

(47) Ngai, K. L.; Roland, C. M. Unusual component dynamics in poly(ethylene oxide)/poly(methyl methacrylate) blends as probed by deuterium NMR. *Macromolecules* **2004**, *37* (8), 2817–2822.

(48) Chen, C. X.; Depa, P.; Sakai, V. G.; Maranas, J. K.; Lynn, J. W.; Peral, I.; Copley, J. R. D. A comparison of united atom, explicit atom, and coarse-grained simulation models for poly(ethylene oxide). *J. Chem. Phys.* **2006**, *124*, 23.

(49) Rault, J. Origin of the Vogel-Fulcher-Tammann law in glass-forming materials: the alpha-beta bifurcation. *J. Non-Cryst. Solids* **2000**, *271* (3), 177–217.
(50) Saboungi, M. L.; Price, D. L.; Mao, G. M.; Fernandez-Perea, R.; Borodin, O.; Smith, G. D.; Armand, M.; Howells, W. S. Coherent neutron scattering from PEO and a PEO-based polymer electrolyte. *Solid State Ionics* **2002**, *147* (3−4), 225–236.
(51) Sakai, V. G.; Maranas, J. K.; Chowdhuri, Z.; Peral, I.; Copley, J. R. D. Miscible blend dynamics and the length scale of local compositions. *J. Polym. Sci., Part B: Polym. Phys.* **2005**, *43* (20), 2914–2923.
(52) Sakai, V. G.; Chen, C. X.; Maranas, J. K.; Chowdhuri, Z. Effect of blending with poly(ethylene oxide) on the dynamics of poly(methyl methacrylate): A quasi-elastic neutron scattering approach. *Macromolecules* **2004**, *37* (26), 9975–9983.
(53) Sacristan, J.; Chen, C. X.; Maranas, J. K. Role of effective composition on dynamics of PEO-PMMA blends. *Macromolecules* **2008**, *41* (14), 5466–5476.
(54) Lin, K.-J.; Maranas, J. K. A molecular dynamics study of ion clustering and movement in poly(ethylene oxide)-based ionomers. Manuscript in preparation.
(55) Graessley, W. W. *Polymeric Liquids & Networks: Structure and Properties*; Taylor & Francis Books, Inc.: New York, 2004.
(56) Tudryn, G. J.; King, D. R.; O'Reilly, M. V.; Winey, K. I. Colby, R. H. Molecular mobility and cation conduction in sulfonated polyester copolymer ionomers. Manuscript in preparation.
(57) Wang, W. Q.; Tudryn, G. J.; Colby, R. H.; Winey, K. I. Thermally driven aggregation in poly(ethylene oxide)-based sulfonate ionomers. *J. Am. Chem. Soc.* **2011**, in press.
(58) Labreche, C.; Levesque, I.; Prudhomme, J. An appraisal of tetraethylsulfamide as plasticizer for poly(ethylene oxide)-LiN-(CF3SO2)(2) rubbery electrolytes. *Macromolecules* **1996**, *29* (24), 7795–7801.
(59) Donth, E. The size of cooperatively rearranging regions at the glass transition. *J. Non-Cryst. Solids* **1982**, *53* (3), 325–330.
(60) Armand, M. Polymer solid electrolytes - an overview. *Solid State Ionics* **1983**, *9−10* (Part 2), 745–754.
(61) Bouridah, A.; Dalard, F.; Deroo, D.; Armand, M. B. Potentiometric measurements of ionic transport parameters in poly(ethylene oxide)-LiX electrolytes. *J. Appl. Electrochem.* **1987**, *17* (3), 625–634.
(62) Eisenberg, A. Clustering of Ions in Organic Polymers. A Theoretical Approach. *Macromolecules* **1970**, *3* (2), 147–154.
(63) Eisenberg, A.; Kim, J.-S. *Introduction to Ionomers*; John Wiley & Sons, Inc.: New York, 1998.
(64) Tant, M. R.; Mauritz, K. A.; Wilkes, G. L. *Ionomers: Synthesis, Structure, Properties and Applications*; Springer: Berlin, 1997.
(65) Maranas, J. K. The effect of environment of local dynamics of macromolecules. *Curr. Opin. Colloid Interface Sci.* **2007**, *12*, 29–42.
(66) Jin, X.; Zhang, S.; Runt, J. Broadband dielectric investigation of amorphous poly(methyl methacrylate)/poly(ethylene oxide) blends. *Macromolecules* **2004**, *37*, 8110–8115.
(67) Bergman, R.; Alvarez, F.; Alegria, A.; Colmenero, J. The merging of the dielectric α- and β-relaxations in poly-(methyl methacrylate). *J. Chem. Phys.* **1998**, *109* (17), 7546–7555.